Electrocatalysis

International Edition: DOI: 10.1002/anie.201705385
German Edition: DOI: 10.1002/ange.201705385

Powder Catalyst Fixation for Post-Electrolysis Structural Characterization of NiFe Layered Double Hydroxide Based Oxygen Evolution Reaction Electrocatalysts

*Corina Andronescu[+], Stefan Barwe[+], Edgar Ventosa, Justus Masa, Eugeniu Vasile, Bharathi Konkena, Sandra Möller, and Wolfgang Schuhmann**

Abstract: *Highly active electrocatalysts for the oxygen evolution (OER) reaction are in most cases powder nanomaterials, which undergo substantial changes upon applying the high potentials required for high-current-density oxygen evolution. Owing to the vigorous gas evolution, the durability under OER conditions is disappointingly low for most powder electrocatalysts as there are no strategies to securely fix powder catalysts onto electrode surfaces. Thus reliable studies of catalysts during or after the OER are often impaired. Herein, we propose the use of composites made from precursors of polybenzoxazines and organophilically modified NiFe layered double hydroxides (LDHs) to form a stable and highly conducting catalyst layer, which allows the study of the catalyst before and after electrocatalysis. Characterization of the material by XRD, SEM, and TEM before and after 100 h electrolysis in 5 M KOH at 60°C and a current density of 200 mA cm^{-2} revealed previously not observed structural changes.*

A major problem in applications of powder (nano)materials as electrocatalysts for energy conversion is caused by the insufficient adherence of the catalyst powder on the electrode surface and the use of often unsuitable binder materials such as Nafion. This is especially difficult at high current densities if the electrocatalytic reaction leads to gas evolution because of the enormous mechanical stress imposed on the often porous particle layer by gas bubble growth and departure. Moreover, commonly used binder materials (such as Nafion) do not provide sufficient electric conductivity and hence prevent fast electron transfer between the catalyst particles and between the particles and the electrode, which causes a substantial decrease in the achievable current density. Moreover, these binder materials do not sustain the high temperatures used during calcination or pyrolysis after electrode modification. Although often overlooked, the durability of those catalysts at the applied high potentials is as important as their activity for the development of potentially technologically viable oxygen evolving electrodes. A decrease in catalytic activity is often observed, but this cannot be unambiguously attributed to catalyst deactivation or degradation of the catalyst film.[1] Thus catalyst powder fixation has to be sufficiently stable that it does not become the limiting factor in the overall electrocatalytic reaction. Consequently, new strategies for the stable immobilization of powder catalysts on electrodes are required not only for their potential future applications, but also for an in-depth evaluation of the intrinsic properties of the catalysts under harsh working conditions and at high current densities.

Recently, we introduced polybenzoxazines (pBOs) as precursors for carbon matrices in which catalyst particles can be stably embedded.[2] Highly crosslinked pBO networks are obtained from the polymerization of benzoxazine (BO) monomers, and show two key features: near-zero volumetric shrinkage during polymerization and the ability to survive thermal treatments under various conditions to yield a large amount of residual char.[3] These properties render pBOs unique and highly suitable for the envisaged catalyst fixation on electrode surfaces. The nature of the carbon obtained after pBO degradation depends strongly on the applied conditions.[4,5] The reported strategy[2] enables the stable immobilization of powder-based catalysts on electrode surfaces while providing improved electron-transfer capabilities.

Layered double hydroxides (LDHs), especially in the form of exfoliated nanosheets,[1,6] supported on carbon nanotubes[7,8] or graphene,[9] or with different metals,[10] have been reported to be among the most active OER catalysts in alkaline media, outperforming state-of-the-art OER catalysts in terms of activity.[11] Detailed studies employing in situ and ex situ characterization techniques have been performed to evaluate the activity and the OER mechanism especially of Ni- and Fe-based LDH materials[12] as well as of ultrathin electrochemically deposited NiFe oxide/hydroxide layers.[13] Stability measurements for NiFe LDHs have been reported

[*] Dr. C. Andronescu,[+] S. Barwe,[+] Dr. E. Ventosa, Dr. J. Masa, Dr. B. Konkena, S. Möller, Prof. Dr. W. Schuhmann
Analytical Chemistry—Center for Electrochemical Sciences
CES, Ruhr-Universität Bochum
44780 Bochum (Germany)
E-mail: wolfgang.schuhmann@rub.de
Dr. C. Andronescu[+]
Advanced Polymer Materials Group
University "Politehnica" of Bucharest
1-7 Gh. Polizu Street, 011061 Bucharest (Romania)
Dr. E. Ventosa
Present address: IMDEA Energy Institute
Avda. Ramón de la Sagra 3, 28935 Móstoles, Madrid (Spain)
Dr. E. Vasile
Departement of Oxide Materials Science and Engineering
University "Politehnica" of Bucharest
1-7 Gh. Polizu Street, 011061 Bucharest (Romania)
[+] These authors contributed equally to this work.
Supporting information and the ORCID identification number(s) for the author(s) of this article can be found under: https://doi.org/10.1002/anie.201705385.

but they were often limited to short periods of time under relatively mild conditions[7,14] and commonly did not include any post-electrolysis characterization (see the Supporting Information, Table S1).

Herein, we report the successful integration of NiFe LDH, one of the most active catalysts for the OER in alkaline media, into a pBO-derived carbon matrix. The catalyst powder adhesion exhibits very high stability even under harsh electrolysis conditions, that is, 200 mA cm^{-2}, 5 M KOH, and 60 °C for 100 h. A detailed characterization of the initial as well as the post-electrolysis catalyst composite material is presented.

The synthesis of a NiFe LDH/pBO composite in which the pBO is intimately incorporated between the layers of the NiFe LDH necessarily requires the interaction of the NiFe LDH with pBO and its monomer BO.[15] We therefore prepared a NiFe LDH containing sodium dodecyl sulfate anions (NiFe SDS) starting from NiFe containing NO_3^- anions (NiFe NO_3; see the Experimental Section in the Supporting Information and Figure S1). NiFe LDH/pBO nanocomposites were then prepared in situ by thermal polymerization of the BO molecules in the presence of the LDH by thermal treatment of their mixtures directly on electrode surfaces. The polymerization step was followed by calcination at 450 °C for 2 h (Scheme 1).

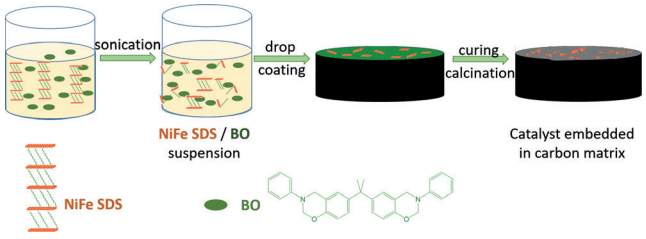

Scheme 1. Preparation of the calcined NiFe LDH/pBO-modified electrode.

Aside from the effect of the calcination, the effect of the pyrolysis of the NiFe LDH/pBO nanocomposites at 450 °C or 600 °C for 2 h under Ar atmosphere on the electrochemical behavior of the NiFe LDH/pBO composite was also investigated (Figure S3). Calcination at 450 °C for 2 h directly after the stepwise polymerization (180 °C/2 h, 200 °C/2 h) of a 3:1 NiFe SDS/BO mixture resulted in the formation of an OER-active composite material (Figure S3) whereas pyrolysis let to a less active catalyst film independent of the applied temperature. The high activity of the calcined sample can be attributed to one of the key features of LDHs, the so-called memory effect.[16] When LDHs are calcined at moderate temperatures, they are able to regenerate their layered structure in the presence of solutions with high OH^- concentrations. On the other hand, LDHs lose this property when pyrolyzed in an inert atmosphere.[17] For all further measurements, samples that had been calcined at 450 °C for 2 h were used.

The memory effect of LDHs can be observed for calcined samples. A calcined NiFe SDS/pBO composite ("NiFe/C") shows two completely distinct diffraction patterns right after the polymerization and calcination (BC = before cycling) and after potential cycling in the presence of OH^- ions (0.1 M KOH; AC = after cycling) as shown in Figure 1. The XRD

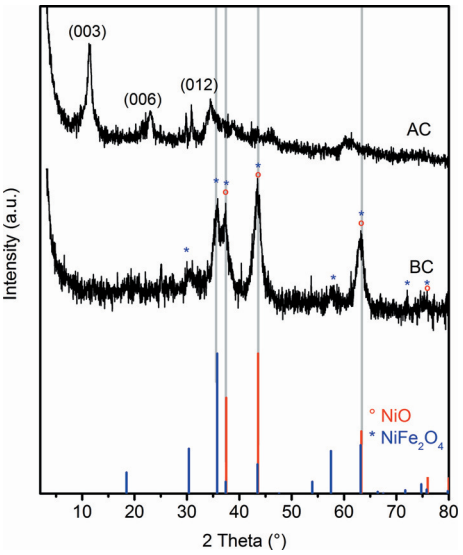

Figure 1. XRD patterns of the calcined NiFe SDS/pBO composite (NiFe/C) before (BC) and after (AC) potential cycling in 0.1 M KOH, and NiO (°) and $NiFe_2O_4$ (*) reference patterns.

pattern of NiFe/C BC shows four major reflections at 2θ = 35.9°, 37.4°, 43.5°, and 63.4°, which can be indexed to the $NiFe_2O_4$ and NiO reference diffraction patterns.[18] No characteristic LDH peaks were observed in the diffraction pattern of the NiFe/C BC sample. However, after 30 min of potential cycling in 0.1 M KOH, the NiFe LDH recovers its layered structure with OH^- as the interlayer anion. The XRD pattern of NiFe/C AC shows again the characteristic LDH reflections at 2θ values of 11.3°, 22.9°, and 34.5°, representing the (003), (006), and (012) reflections, respectively (Figure 1 and Figure S1). The basal plane spacing of the recovered NiFe LDH of 0.75 nm is clearly smaller than that of NiFe NO_3 (1.02 nm) owing to the presence of OH^- and CO_3^{2-} anions inside the galleries.[19]

During calcination, the highly crosslinked pBO network is converted into amorphous carbon as manifested by the typical D and G bands of carbon at Raman shifts of 1350 cm^{-1} and 1590 cm^{-1}, respectively (Figure S4).[4] The transformation of the pBO network into carbon is a very crucial step for the creation of the necessary catalyst immobilization matrix with high electric conductivity. Otherwise, pBO would act as an insulator. TEM images show that upon calcination (NiFe/C BC), nanometric particles of different sizes are embedded in a carbon matrix (Figure 2a and Figure S5a–c). The selected area electron diffraction (SAED) pattern (Figure S5d) shows features that are characteristic for $NiFe_2O_4$ and NiO.

After potential cycling in 0.1 M KOH, the material adopts a clearly different structure. TEM analysis revealed the presence of layers, confirming the regeneration of the layered

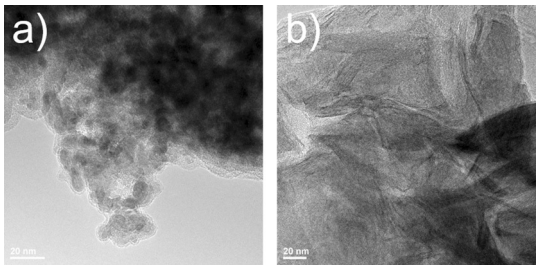

Figure 2. HRTEM images of NiFe/C a) as prepared (NiFe/C BC) and b) after potential cycling in 0.1 M KOH (NiFe/C AC).

structure after introduction of the mixed oxides into the OH^- containing solution (Figure 2b and Figure S6). Aside from the LDH layers, discrete NiO nanoparticles were also observed in the carbon matrix (see the SAED images in Figure S6), indicating that $NiFe_2O_4$ had most likely been transformed into NiFe LDH. XPS survey spectra confirmed the presence of carbon in NiFe/C both before and after cycling (Figure S7), which is in good agreement with the Raman results, and confirmed the presence of Ni in its +2 oxidation state (Figure S8), while Fe is present as Fe^{3+} (Figure S9). Sufficient evidence can thus be derived from the XRD, TEM, and XPS results to confirm that at least partial regeneration of the LDH structure occurs upon electrochemical cycling of the calcined sample.

NiFe NO_3 delivered outstanding electrochemical properties towards the OER in accordance with literature values, requiring an overpotential of only 0.27 V to reach a current density of 10 mA cm^{-2} with a low Tafel slope of around 56 mV dec^{-1} (Figure 3a). Hydrodynamic voltammetry in O_2-saturated KOH (0.1M) revealed a slightly lower activity of NiFe SDS as compared to NiFe NO_3, with an overpotential of 0.29 V to reach a current density of 10 mA cm^{-2} (Figure 3a). The Tafel slope of NiFe SDS changed from 59 mV dec^{-1} in the lower current density region to 150 mV dec^{-1} at higher current densities, indicating a change in the OER mechanism (Figure 3b).

The slightly lower activity of NiFe SDS can be explained by the larger interlayer spacing caused by the larger organic anions, which decreases the electronic conductivity between the single layers.[1] The initial OER activity of NiFe/C (NiFe SDS/BO monomer = 3:1) before cycling (NiFe/C BC) was lower than that of NiFe NO_3 (Figure 3a). The calcined material afforded 10 mA cm^{-2} at an overpotential of 0.35 V, which is 0.06 V higher than the value attained for NiFe NO_3 (0.29 V). The initial Tafel slope of NiFe/C BC (59 mV dec^{-1}; Figure 3b) was similar to that of NiFe NO_3. A stability test by consecutive voltammetric scans revealed the poor stability of both NiFe NO_3 as well as NiFe SDS (Figure S10a,b). In the course of fast potentiodynamic cycling during 50 CVs, the activity of both LDHs decreased drastically while it remained essentially unchanged for the NiFe/C nanocomposite (Figure S10c). NiFe NO_3 still showed an early OER onset, but the overpotential needed to afford 10 mA cm^{-2} increased to 0.32 V. The increase in the current density with the potential substantially decreased, suggesting poor electric conductivity in the catalyst layer. The activity of NiFe SDS declined even more, and the overpotential to reach the same current density increased to 0.4 V, while NiFe/C AC required an overpotential of only 0.33 V to reach 10 mA cm^{-2} (Figure 3c). Additionally, the Tafel slope increased significantly after potential cycling to 158 mV dec^{-1} and 131 mV dec^{-1} for NiFe NO_3 and NiFe SDS, respectively (Figure 3d). The Tafel slope of NiFe/C remained unchanged (57 mV dec^{-1}) upon potential cycling (Figure 3d). The lower Tafel slope of NiFe/C compared to NiFe NO_3 and NiFe SDS after potential cycling can be attributed to the enhanced stability as well as the favorable electronic conductivity of the catalyst film provided by the pBO-derived carbon matrix. The Faradaic efficiency was close to 100% (98.3%), and differential electrochemical mass spectrometry (DEMS) revealed oxygen as the only reaction product (see the Experimental Section in the Supporting Information and Figures S11 and S12).

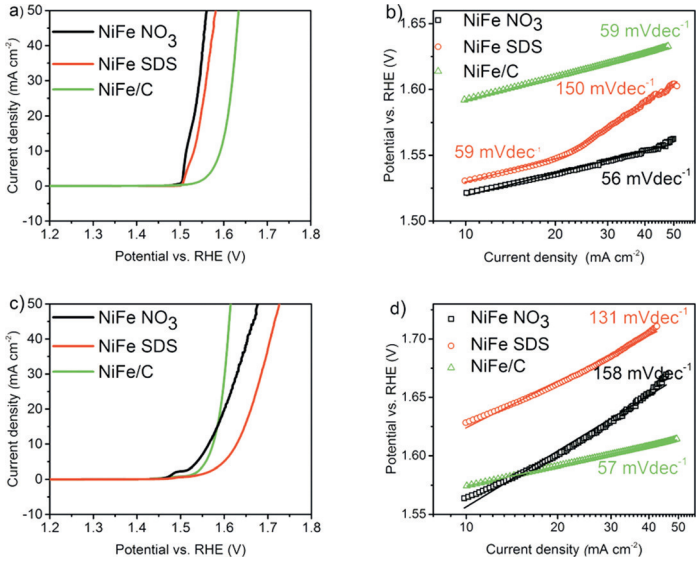

Figure 3. Linear sweep voltammograms recorded in O_2-saturated KOH (0.1 M) at a scan rate of 5 mV s^{-1} and 1600 rpm electrode rotation, showing OER electrocatalysis at NiFe NO_3 (black), NiFe SDS (red), and NiFe/C (green) modified electrodes before (a) and after (c) potentiodynamic cycling. Tafel slopes of NiFe NO_3 (black squares), NiFe SDS (red circles), and NiFe/C (green triangles) before (b) and after (d) potentiodynamic cycling.

A preliminary stability test conducted following an accelerated stability test procedure (Figure 4a)[20] using catalyst-modified graphite paper electrodes in a flow-through electrochemical cell with O_2-saturated 0.1M KOH as the electrolyte (Figure S13 and the Methods Section in the Supporting Information) was performed for NiFe NO_3 as well as NiFe/C. During 48 consecutive cycles of galvanostatic polarization, the potential required to maintain a current density of 50 mA cm^{-2} for NiFe NO_3 fluctuated but increased from 1.69 V vs. RHE in the first cycle to 1.84 V vs. RHE after the 48th cycle (Figure 4a).

The potential of NiFe/C was 1.76 V vs. RHE in the first cycle and remained virtually unchanged after the 48th cycle (Figure 4a). These results evidently demonstrate that despite the impressive OER activity of NiFe

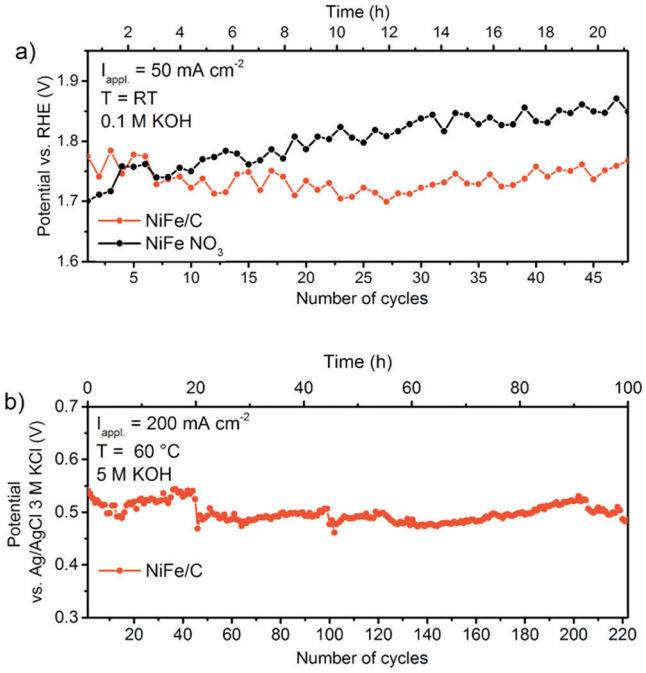

Figure 4. a) Potential versus cycle number for NiFe NO_3 (black) and NiFe/C (red), with each point representing the potential after 450 s during galvanostatic polarization in 0.1 M KOH at room temperature at an applied current density of 50 mA cm^{-2}. b) Potential versus cycle number for NiFe/C (red), with each point representing the potential at 450 s during galvanostatic polarization in 5 M KOH at 60 °C at an applied current density of 200 mA cm^{-2}.

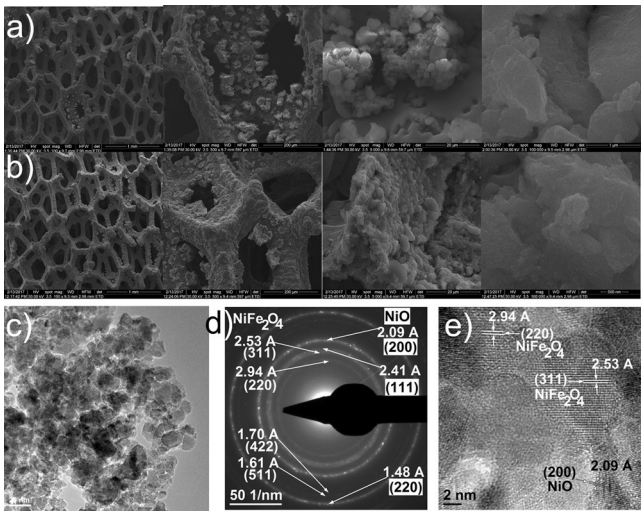

Figure 5. SEM images of NiFe/C prepared on Ni foam before (a) and after (b) electrolysis for 100 h at a current density of 200 mA cm^{-2} in 5 M KOH and at 60 °C at different magnifications: 100×, 500×, 5000×, and 100000× (from left to right). c, e) HRTEM images of the NiFe/C catalyst deposited on Ni foam after 100 h of OER in 5 M KOH at 60 °C and 200 mA cm^{-2}. d) SAED pattern of (c).

NO_3, its durability would suffice neither for detailed investigation after several days of electrolysis nor for potentially envisaged applications. The comparably poor stability of NiFe NO_3 may be caused either by (electro)chemical deactivation or by detachment of the catalyst from the electrode surface. The enhanced long-term stability of NiFe/C is due to its improved immobilization on the electrode surface, indicating that in the case of NiFe NO_3, detachment of the catalyst from the electrode could be the major cause of its faster activity loss. As the NiFe/C nanocomposite catalyst demonstrated very promising stability over a period of 21 h, we performed a NiFe/C durability test under even harsher conditions, that is, in 5 M KOH at 60 °C and a current density of 200 mA cm^{-2}. For this test, NiFe/C was prepared on Ni foam as Ni is one of the mostly used electrode materials in alkaline electrolysis.[21] The potential to afford a current density of 200 mA cm^{-2} fluctuates constantly around a value of 0.5 V vs. Ag/AgCl/3 M KCl during 100 h (Figure 4b). Owing to faster electrolyte evaporation at 60 °C, the potential slightly increased during the night while it decreased upon readjusting the electrolyte volume during the day. Detailed characterization of the catalyst after the electrochemical experiments was performed by SEM-EDX, TEM, XRD, and XPS. The SEM images presented in Figure 5a, b do not show any significant change in the catalyst morphology after operating at 200 mA cm^{-2} for 100 h (5 M KOH, 60 °C).

High-resolution C 1s XPS spectra of NiFe/C before and after 100 h of electrolysis both show a mixture of signals for C–C bonds and oxidized carbon (Figure S16). No significant difference can be observed between the two samples, indicating that the nature of the carbon did not change during the OER. XRD patterns obtained from NiFe/C directly prepared on Ni foam and after the 100 h durability test show the characteristic diffraction patterns of Ni and NiO from the Ni foam support.[23] Additionally, three very small peaks are observed at $2\theta = 30°$, 35.7°, and 57.2° which are characteristic of $NiFe_2O_4$. No characteristic peak for the LDH can be seen (Figure S17). Moreover, TEM shows that after the 100 h durability test at elevated temperature, NiFe/C has been converted into a mixture of NiO and $NiFe_2O_4$ nanoparticles (Figure 5c–e). Evidently, during 100 h of OER at high current densities and high temperatures, the catalyst is transformed into a spinel structure, which has not been reported yet for LDH-based electrocatalysts. The transformation of LDHs into their corresponding spinel structures at temperatures between 60 to 95 °C in aqueous media has, however, already been described for other types of LDH.[22] In addition, it is known that the NiFe catalyst structure changes when high anodic potentials are applied as required for the OER.[12] Evidently, the proposed tight fixation of the NiFe LDH within the pBO-derived carbon matrix not only provides the possibility to investigate the long-term stability of the powder catalyst without its detachment from the electrode surface but also guarantees sufficient stability even at high electrolyte concentrations, high temperatures, and high applied current densities (5 M KOH, 60 °C, 200 mA cm^{-2}) as the basis for post-electrochemistry structure characterization. The transformation of an NiFe LDH during the OER at higher temperatures has not been described before.

In conclusion, we have described the formation of a highly active and stable catalyst (NiFe/C) for the OER by calcination of a nanocomposite of a NiFe LDH and a polybenzoxazine-based resin. The highest catalytic activity was obtained using a 3:1 ratio of NiFe SDS and the BO monomer. XRD,

XPS, and TEM analysis showed that the final catalyst material consisted of a NiFe LDH as well as NiO embedded in a carbon matrix. The calcined nanocomposite was electrochemically activated by potential cycling in aqueous 0.1M KOH, which led to the regeneration of the NiFe LDH structure. Using this approach, NiFe LDH layers embedded in an electrically conducting and stable carbon matrix were directly formed on electrode surfaces, providing very stable and active OER catalyst films. NiFe/C directly prepared on Ni foam demonstrated a highly stable electrochemical response in 5M KOH at 60°C and 200 mA cm^{-2} for 100 h. Although the NiFe/C catalyst is transformed from a NiFe LDH into a mixture of NiO and Ni_2FeO_4 nanoparticles during the OER at high temperatures, the catalyst film is still attached to the electrode, showing the feasibility of the suggested approach for fixing powder catalysts onto electrode surfaces.

Acknowledgements

We are grateful to the Deutsche Forschungsgemeinschaft (DFG) for funding within the framework of the Cluster of Excellence "Resolv" (EXC1069) and the Bundesministerium für Bildung und Forschung (BMBF) for funding within the framework of the project "Mangan" (FKZ 03EK3548).

Conflict of interest

The authors declare no conflict of interest.

Keywords: catalyst stability · electrocatalysis · layered double hydroxides · polybenzoxazine · water oxidation

How to cite: *Angew. Chem. Int. Ed.* **2017**, *56*, 11258–11262
Angew. Chem. **2017**, *129*, 11411–11416

[1] F. Song, X. Hu, *Nat. Commun.* **2014**, *5*, 4477.
[2] S. Barwe, C. Andronescu, J. Masa, E. Ventosa, S. Klink, A. Genc, J. Arbiol, W. Schuhmann, *ChemSusChem* **2017**, *10*, 2653.
[3] a) H. Y. Low, H. Ishida, *Polymer* **1999**, *40*, 4365; b) C. H. Lin, S. X. Cai, T. S. Leu, T. Y. Hwang, H. H. Lee, *J. Polym. Sci. Part A* **2006**, *44*, 3454; c) H. Zhang, W. Gu, R. Zhu, Q. Ran, Y. Gu, *High Temp. Mater. Processes* **2015**, *34*, 245; d) K. Hemvichian, H. Ishida, *Polymer* **2002**, *43*, 4391.
[4] M. Sevilla, A. B. Fuertes, *Carbon* **2013**, *56*, 155.
[5] L. Wan, J. Wang, Y. Sun, C. Feng, K. Li, *RSC Adv.* **2015**, *5*, 5331.
[6] a) F. Song, X. Hu, *J. Am. Chem. Soc.* **2014**, *136*, 16481; b) B. M. Hunter, J. D. Blakemore, M. Deimund, H. B. Gray, J. R. Winkler, A. M. Muller, *J. Am. Chem. Soc.* **2014**, *136*, 13118.
[7] M. Gong, Y. Li, H. Wang, Y. Liang, J. Z. Wu, J. Zhou, J. Wang, T. Regier, F. Wei, H. Dai, *J. Am. Chem. Soc.* **2013**, *135*, 8452.
[8] R. Chen, G. Sun, C. Yang, L. Zhang, J. Miao, H. Tao, H. Yang, J. Chen, P. Chen, B. Liu, *Nanoscale Horiz.* **2016**, *1*, 156.
[9] a) X. Long, J. Li, S. Xiao, K. Yan, Z. Wang, H. Chen, S. Yang, *Angew. Chem. Int. Ed.* **2014**, *53*, 7584; *Angew. Chem.* **2014**, *126*, 7714; b) D. H. Youn, Y. B. Park, J. Y. Kim, G. Magesh, Y. J. Jang, J. S. Lee, *J. Power Sources* **2015**, *294*, 437; c) W. Ma, R. Ma, C. Wang, J. Liang, X. Liu, K. Zhou, T. Sasaki, *ACS Nano* **2015**, *9*, 1977.
[10] a) X. Long, S. Xiao, Z. Wang, X. Zheng, S. Yang, *Chem. Commun.* **2015**, *51*, 1120; b) K. Fan et al., *Nat. Commun.* **2016**, *7*, 11981.
[11] a) X. Long, Z. Wang, S. Xiao, Y. An, S. Yang, *Mater. Today* **2016**, *19*, 213; b) G. Fan, F. Li, D. G. Evans, X. Duan, *Chem. Soc. Rev.* **2014**, *43*, 7040.
[12] a) D. Friebel et al., *J. Am. Chem. Soc.* **2015**, *137*, 1305; b) J. Y. C. Chen, L. Dang, H. Liang, W. Bi, J. B. Gerken, S. Jin, E. E. Alp, S. S. Stahl, *J. Am. Chem. Soc.* **2015**, *137*, 15090; c) F. Dionigi, P. Strasser, *Adv. Energy Mater.* **2016**, 1600621.
[13] a) M. W. Louie, A. T. Bell, *J. Am. Chem. Soc.* **2013**, *135*, 12329; b) L. Trotochaud, S. L. Young, J. K. Ranney, S. W. Boettcher, *J. Am. Chem. Soc.* **2014**, *136*, 6744; c) W. Zhang, Y. Wu, J. Qi, M. Chen, R. Cao, *Adv. Energy Mater.* **2017**, *7*, 1602547.
[14] a) X. Yu, M. Zhang, W. Yuan, G. Shi, *J. Mater. Chem. A* **2015**, *3*, 6921; b) S. Dresp, F. Luo, R. Schmack, S. Kühl, M. Gliech, P. Strasser, *Energy Environ. Sci.* **2016**, *9*, 2020; c) X. Long, J. Li, S. Xiao, K. Yan, Z. Wang, H. Chen, S. Yang, *Angew. Chem.* **2014**, *126*, 7714; *Angew. Chem.* **2014**, *126*, 7714.
[15] C. Andronescu, S. A. Garea, E. Vasile, H. Iovu, *Compos. Sci. Technol.* **2014**, *95*, 29.
[16] P. Kowalik, M. Konkol, M. Kondracka, W. Próchniak, R. Bicki, P. Wiercioch, *Appl. Catal. A* **2013**, *464–465*, 339.
[17] a) F. R. Costa, A. Leuteritz, U. Wagenknecht, D. Jehnichen, L. Häußler, G. Heinrich, *Appl. Clay Sci.* **2008**, *38*, 153; b) B. Zümreoglu-Karan, A. Ay, *Chem. Pap.* **2012**, *66*, 1.
[18] a) J. Qi, W. Zhang, R. Xiang, K. Liu, H.-Y. Wang, M. Chen, Y. Han, R. Cao, *Adv. Sci.* **2015**, *2*, 1500199; b) W. Zhang, J. Qi, K. Liu, R. Cao, *Adv. Energy Mater.* **2016**, *6*, 1502489.
[19] B. M. Hunter, W. Hieringer, J. R. Winkler, H. B. Gray, A. M. Müller, *Energy Environ. Sci.* **2016**, *9*, 1734.
[20] A. Maljusch, O. Conradi, S. Hoch, M. Blug, W. Schuhmann, *Anal. Chem.* **2016**, *88*, 7597.
[21] J. D. Holladay, J. Hu, D. L. King, Y. Wang, *Catal. Today* **2009**, *139*, 244.
[22] Q. Xu, Y. Wei, Y. Liu, X. Ji, L. Yang, M. Gu, *Solid State Sci.* **2009**, *11*, 472.
[23] D. Guo, J. Qi, W. Zhang, R. Cao, *ChemSusChem* **2017**, *10*, 394.

Manuscript received: May 25, 2017
Revised manuscript received: June 15, 2017
Accepted manuscript online: June 25, 2017
Version of record online: August 11, 2017

